Systems/Circuits

Glucagon-Like Peptide-1 Receptors in the Gustatory Cortex Influence Food Intake

Amanda M. Dossat,* Milayna M. Kokoska,* Jessica R. Whitaker-Fornek,* Sarah E. Sniffen, Aishwarya S. Kulkarni, Erica S. Levitt, and Daniel W. Wesson

Department of Pharmacology and Therapeutics, University of Florida College of Medicine, Gainesville, Florida 32610

The gustatory cortex (GC) region of the insular cortex processes taste information in manners important for taste-guided behaviors, including food intake itself. In addition to oral gustatory stimuli, GC activity is also influenced by physiological states including hunger. The specific cell types and molecular mechanisms that provide the GC with such abilities are unclear. Glucagon-like peptide 1 (GLP-1) is produced by neurons in the brain, where it can act on GLP-1 receptor-expressing (GLP-1R+) neurons found in several brain regions. In these brain regions, GLP-1R agonism suppresses homeostatic food intake and dampens the hedonic value of food. Here, we report in mice of both sexes that cells within the GC express *Glp1r* mRNA and further, by *ex vivo* brain slice recordings, that GC GLP-1R+ neurons are depolarized by the selective GLP-1R agonist, exendin-4. Next we found that chemogenetic stimulation of GLP-1R+ neurons, and also pharmacological stimulation of GC-GLP-1Rs themselves, both reduced homeostatic food intake. When mice were chronically maintained on diets with specific fat contents and then later offered foods with new fat contents, we also found that GLP-1R agonism reduced food intake toward foods with differing fat contents, indicating that GC GLP-1R influences may depend on palatability of the food. Together, these results provide evidence for a specific cell population in the GC that may hold roles in both homeostatic and hedonic food intake.

Key words: **feeding; gustation; ingestive behavior**

Significance Statement

The present study demonstrates that a population of neurons in the GC region of the insular cortex expresses receptors for GLP-1Rs, these neurons are depolarized by agonism of GLP-1Rs, and GC GLP-1Rs can influence food intake on their activation, including in manners depending on food palatability. This work is significant by adding to our understanding of the brain systems that mediate ingestive behavior, which holds implications for metabolic diseases.

Introduction

The gustatory region of the insular cortex (GC) is a brain region wherein tastant information is processed in manners critical for taste-guided behaviors, including food intake and the development of taste preferences. In line with this role, GC activity in animals ranging from mice and rats to humans can reflect the perceived palatability of tastes (Katz et al., 2001; Small et al., 2001; Accolla and Carleton, 2008; Sadacca et al., 2012, 2016; Jezzini et al., 2013; Bouaichi and Vincis, 2020; Vincis et al., 2020). The GC is a highly innervated cortical region (Gehrlach et al., 2020) that receives projections from gustatory and visceral-associated brain regions (Livneh et al., 2017, 2020; Di Lorenzo, 2021). The GC also receives input from brain areas that may influence the desire to eat (Di Lorenzo, 2021) and importantly projects to brain areas involved in regulating food intake (Yasui et al., 1991; Zhang et al., 2009; Wu et al., 2020; Samuelsen and Vincis, 2021).

In addition to orosensory information, the GC is also sensitive to metabolic status, wherein GC neurons are more active during hunger versus satiety (Small et al., 2001; Hinton et al., 2004; de Araujo et al., 2006; Malik et al., 2008; Livneh et al., 2017). Beyond processing taste and interoceptive information, manipulation of GC activity alters ingestive behavior (Baldo et al., 2016; Stern et al., 2020, 2021; Wu et al., 2020; Zhang-Molina et al., 2020). Together, the GC is positioned to modulate

Received Aug. 31, 2022; revised Apr. 5, 2023; accepted Apr. 19, 2023.

Author contributions: A.M.D., M.M.K., J.W.-F., S.E.S., E.S.L., and D.W.W. designed research; A.M.D., M.M.K., J.W.-F., S.E.S., A.S.K., E.S.L., and D.W.W. performed research; A.M.D., M.M.K., J.W.-F., S.E.S., and E.S.L. analyzed data; and A.M.D. and D.W.W. wrote the paper.

This work was supported by University of Florida Research Opportunity Seed Fund 00130743 to A.M.D. and D.W.W., National Institutes of Health (NIH) Grant R01DA047978 to E.S.L., and NIH Grants R01DC014443, R01DA049545, and R01DC016519 to D.W.W. S.E.S. was supported by NIH–National Institute on Deafness and Other Communication Disorders Grant T32015994. We thank Drs. Minghong Ma, Alan Spector, Alfredo Fontanini, and Steven Munger for discussions during this project.

*A.M.D., M.M.K., and J.W.-F. share first authorship.

The authors declare no competing financial interests.

Correspondence should be addressed to Daniel W. Wesson at danielwesson@ufl.edu.

https://doi.org/10.1523/JNEUROSCI.1668-22.2023

ingestive behavior via integration of gustatory and visceral signals (Katz et al., 2001, 2002; Maffei et al., 2012), including those arising from the enteroinsular axis (Unger and Eisentraut, 1969). Although there is both preclinical and clinical evidence supporting the role of the GC as a key interoceptive brain region, the cellular mechanisms remain poorly understood.

Taste-related information is transmitted to the brain via signals arising from the mouth, whereas meal-related interoceptive information is conveyed via signals from within the gut. This concert of signals allows one to experience hunger/fullness and control ingestion. There are many peptides that influence ingestive behavior (Crespo et al., 2014; Gautron et al., 2015). For example, the gut signals fullness (e.g., gastric stretch) through the secretion of meal-related peptides such as the enteroinsular axis modulator Glucagon-like peptide 1 (GLP-1; Creutzfeldt, 2001), which can bind to GLP-1 receptors (GLP-1Rs on the vagus nerve (Williams et al., 2016). The nucleus of the solitary tract contains a population of GLP-1-producing neurons that are activated by gastric stretch (Vrang et al., 2003), leptin (Hisadome et al., 2010), and cholecystokinin (Hisadome et al., 2011). These neurons send projections to feeding-relevant brain regions that express GLP-1Rs (Larsen et al., 1997; Merchenthaler et al., 1999; Vrang et al., 2007), which include the hypothalamus (Larsen et al., 1997; Rinaman, 2010), nucleus accumbens (Dossat et al., 2011; Alhadeff et al., 2012), and the lateral septum (Terrill et al., 2019), among others, wherein GLP-1R agonists reduce food intake (Tang-Christensen et al., 1996; McMahon and Wellman, 1998; Dossat et al., 2011; Kanoski et al., 2011; Alhadeff et al., 2012). The precise mechanism through which GLP-1R agonism influences ingestive behavior seems to depend in-part on the brain region where GLP-1Rs are expressed. For example, hypothalamic GLP-1R activation suppresses homeostatic food intake (McMahon and Wellman, 1998), whereas GLP-1R activation within the nucleus accumbens dampens the hedonic value of food (Dickson et al., 2012; Dossat et al., 2013; López-Ferreras et al., 2018). The food intake-reducing effects of GLP-1R agonism is influenced by consumption and maintenance on a high-fat (HF) diet (Williams et al., 2011; Duca et al., 2013). During investigations into other brain regions, we serendipitously observed expression of *Glp1r* mRNA in the GC, which raised the exciting possibility that GLP-1 acts on GC neurons to provide its well-established influence on ingestive behavior.

Here, we used a combination of fluorescent *in situ* hybridization, immunohistochemistry, *ex vivo* electrophysiology, chemogenetics, and behavioral pharmacology to investigate a possible role for GLP-1Rs in the GC. We aimed to answer the following questions: Where are GLP-1Rs expressed in the GC? Are there anatomic or cortical layer-specific expression of GLP-1Rs? Are GLP-1R+ neurons responsive to GLP-1R ligands? Does agonism of GC GLP-1Rs influence food intake? And finally, because of the known application of GLP-1R analogues as therapeutics for obesity (Wilding et al., 2021), does the possible influence of these receptors change when metabolic state changes, like in the case of chronic high-fat diet, and/or because of palatability of food?

Materials and Methods

Animals. Adult C57BL/6J mice (N = 51; 27 males, 18 females) bred in a University of Florida vivarium from breeder stock originating from The Jackson Laboratory ($Glp1r^{tm1.1(cre)Lbrl}$ heterozygotes; Williams et al., 2016; N = 24; 10 males, 14 females; Glp1r-Cre; strain #029283, The Jackson Laboratory), and Glp1r-Cre heterozygotes crossed with homozygotic B6.Cg-Gt(ROSA)26Sortm9(CAG-tdTomato)Hze/J mice (strain #007909, The Jackson Laboratory, Madisen et al., 2010; N = 15; 12 males, three females; Glp1r-Cre;Ai9) were used in the present study. Mice were housed in a temperature-controlled vivarium on a 12 h light/dark cycle with *ad libitum* access to water and rodent chow (catalog #2018, Teklad, and catalog #2918, Envigo), except where otherwise stated. All of the experimental procedures were conducted in accordance with the guidelines from the National Institutes of Health and approved by the University of Florida Institutional Animal Care and Use Committee.

RNAscope fluorescent in situ *hybridization.* C57BL/6J mice were anesthetized with Fatal Plus (100 mg/kg; catalog #002989373-68, Vortech Pharmaceuticals) and transcardially perfused with chilled 0.9% saline. Brains were quickly removed (<5 min), flash frozen in isopentane (catalog #AC126470010, Thermo Fisher Scientific) on dry ice, and stored at −80°C until further processing. Coronal sections (10 μM) were cryosectioned at −20°C, mounted onto SuperFrost Plus slides (catalog #12-550-15, Thermo Fisher Scientific), and fluorescent *in situ* hybridization (FISH) experiments were performed according to the protocol from the manufacturer for fresh-frozen samples using the RNAscope Multiplex Fluorescent v2 assay (catalog #323136, Advanced Cell Diagnostics; Wang et al., 2012). The probe for *Glp1r* (catalog #418851) was paired with the Opal fluorophore 690 (catalog #NC1605064, Akoya Biosciences). The 3-Plex Negative Control Probe (dapB, catalog #320871, Advanced Cell Diagnostics) and the positive control probe (polymerase II subunit RPB1, Peptidyl-prolyl *cis*-trans isomerase B, and ubiquitin C, catalog #300041, Advanced Cell Diagnostics) were processed in parallel with the target probes to confirm assay performance and RNA integrity of the samples.

Immunohistochemistry. Glp1r-Cre;Ai9 mice were transcardially perfused with chilled 0.9% saline followed by 10% neutral buffered formalin (catalog #SF100-4, Thermo Fisher Scientific). Brains were removed and postfixed 24 h at 4°C in 30% sucrose in 10% buffered formalin. Serial coronal sections (40 μM) from frozen brains were taken throughout the GC on a Leica microtome and stored in PBD in 0.3% sodium azide. Sections were rinsed 3× (5 min each) in Tris-buffered saline (TBS) and blocked in 5% normal goat serum (catalog #G9023, Millipore) for 1 h at room temperature. Next, sections were incubated in rabbit anti-NeuN, (1:1000; catalog #ab177487, Abcam) for 24 h at 4°C. Sections were then rinsed 3× for 10 min in TBS and incubated in goat anti-rabbit IgG 488 (1:1000; catalog #A11034, Invitrogen) for 2 h at room temperature. Finally, sections were rinsed 3× (5 min each) in TBS and 3× in ddH20 before mounting sections on slides (catalog #12-550-433, Thermo Fisher Scientific). The sections were treated with DAPI-supplemented mounting medium (DAPI Fluoromount-G, catalog #OB010020, SouthernBiotech) and coverslipped.

Imaging and quantification. Brain regions of interest (ROIs) were identified using the DAPI signal referenced to a mouse brain atlas (Paxinos and Franklin, 2000). Immunofluorescence was detected and imaged using an upright epifluorescent microscope (Nikon Ti2e ECLIPSE) at 10, 20, or 40× magnification. For FISH and immunohistochemical analyses, ROIs were drawn around the GC or nucleus accumbens (NAc) to allow for restricted quantification of the fluorescent signal within those areas of interest. For quantification, semiautomated recipes were used to produce counts of the signal(s) of interest based on fluorescence intensity, size, and localization to a given ROI. Gain, exposure, and light brightness were held consistent across brain regions and animals to allow for accurate comparisons.

Brain slice electrophysiology. Ex vivo brain slice recordings were performed in Glp1r-Cre;Ai9 mice wherein tdTomato expression is directed within cells expressing Glp1r. Mice (n = 9) were anesthetized with isoflurane (4%) and rapidly decapitated. Brains were removed, blocked, and mounted in a vibratome chamber (Leica VT 1200S). Coronal slices (230 μm) containing the GC (1.7 mm anterior bregma, ~2–5; 3 mm lateral, identified based on anatomic coordinates; Paxinos and Franklin, 2000) were collected in room-temperature artificial CSF (aCSF) that contained the following (in mM): 126 NaCl, 2.5 KCl, 1.2 MgCl2, 2.4 CaCl2, 1.2 NaH_2PO_4, 11 D-glucose, and 21.4 NaHCO3 (equilibrated with 95% O_2/5% CO_2). Slices were stored at 32°C in glass vials with carbogen-equilibrated aCSF. MK801 (10 μM) was added to the cutting solution and for the initial incubation of slices in storage (at least 30 min) to block NMDA-receptor-mediated excitotoxicity. Following incubation,

the slices were transferred to a recording chamber that was perfused with equilibrated aCSF warmed to 34°C (Warner Instruments) at a flow rate of 1.5–3 ml/min. Cells were visualized using an upright microscope (Nikon FN1) equipped with custom-built infrared (IR)-Dodt gradient contrast illumination and a DAGE-MTI IR-1000 camera. Fluorescence was identified using LED epifluorescence illumination with a Texas Red filter cube (excitation, 559 nM; emission, 630 nM) and detected using a DAGE-MTI IR-1000 camera with sufficient sensitivity in the tdTomato emission range. We targeted and recorded from tdTomato-positive (tdTomato+) neurons as GLP-1R+ neurons and nearby tdTomato-negative neurons as GLP-1R-null (GLP-1RØ). Whole-cell recordings from layers II/III GC neurons were performed with an MultiClamp 700B amplifier (Molecular Devices) in voltage-clamp (Vhold = −60 mV) or current-clamp mode. Recording pipettes (1.5–2.5 MΩ) were filled with internal solution that contained the following (in mM): 115 potassium methanesulfonate, 20 NaCl, 1.5 MgCl2, 5 HEPES(K), 2 BAPTA, 1–2 Mg-ATP, 0.2 Na-GTP, adjusted to 7.35 pH, and 275–285 mOsM. Liquid junction potential (10 mV) was not corrected. Data were low-pass filtered (10 kHz) and sampled at 20 kHz with pCLAMP 11.1 software, or at 400 Hz with PowerLab software (LabChart version 8.1.16). To block excitatory and inhibitory fast synaptic transmission, strychnine (1 μM), picrotoxin (100 μM), and DNQX (10 μM; all from Sigma-Aldrich) were added to the aCSF. Current-voltage (*I–V*) relationships were determined with a series of 10 mV voltage steps (−50 to −140 mV) at baseline and during perfusion of the high affinity GLP-1R agonist Exendin-4 (Ex-4; 100 nM; catalog #4044219, Bachem). The baseline *I–V* was subtracted from the *I–V* during Ex-4 to determine the reversal potential of the Ex-4-mediated current. Action potential data were acquired in current-clamp mode by injecting current steps (−50 to +400 pA, 500 ms). Series resistance was monitored without compensation and remained <20 MΩ for inclusion. All drugs were applied by bath perfusion at the indicated concentrations.

Surgical procedures. In all surgeries, mice were anesthetized with isoflurane (4% induction, 2% maintenance; IsoFlo, Patterson Veterinary) in 1 L/min O_2 and head fixed in a stereotaxic frame (model 1900, Kopf Instruments) with the torso lying on a water bath heating pad (38°C). Following injection of local anesthetic (bupivacaine, 5 mg/kg; Patterson Veterinary) into the scalp and a midline incision along the skull cap, craniotomies were made bilaterally above the GC (1.7 mm anterior bregma, 2.4 mm lateral midline; Paxinos and Franklin, 2000).

For DREADD-based chemogenetic manipulation (Armbruster et al., 2007) of GC GLP-1R+ neurons, adeno associated virus (AAV)8-hSyn-DIO-HA-hM3D(Gq)-IRES-mCitrine (AAV-DIO-hM3D (Gq)-mCitrine, 2.3×10^{13} vg/ml, 200 nl/hemisphere; catalog #50454-AAV8, Addgene) or AAV5-EF1a-DIO-eYFP (AAV-DIO-eYFP, 1×10^{12} vg/ml, 100 nl/hemisphere; catalog #27056-AAV5, Addgene) for control was delivered bilaterally into the GC of Glp1r-Cre mice at the coordinates above at a depth of 2 mm ventral from the brain surface. Following infusion, the micropipette was slowly withdrawn from the brain. The craniotomies were sealed with wax and the scalp closed with Vetbond (3M).

For pharmacological manipulation of GC GLP-1Rs, bilateral craniotomies were made above the GC, and miniature guide cannulae (catalog #C315GMN/SPC, P1 Technologies) extending 2.25 mm beyond pedestal were implanted at the coordinates above at a depth of 1.8 mm ventral. Cannulae were secured to the skull by Vetbond followed by dental cement, and dust caps with a 2.05 mm projection wire were inserted.

For both AAV injections and cannulations, mice recovered on a heating pad until ambulatory and then were single housed. Cannulated mice and AAV-injected mice were given 7 and 14 d, respectively, after surgery to recover before the onset of acclimation to behavioral procedures. Meloxicam analgesic (5 mg/kg, s.c.) was administered for at least 3 d following surgery.

Food intake experiments. Mice were habituated to handling and dark-cycle food intake measurements on at least two occasions before testing to minimize the effects of stress on food intake. Food intake measures were performed by experimenters A.M.D., M.M.K., S.E.S., and A.E.K, with M.M.K., S.E.S., and A.E.K. blind to the treatment conditions. When mice exhibited <15% variation in food intake across days, they were considered habituated. Food was removed from cages 2 h before dark-cycle onset, and initial food weight and body weight were recorded at this time. To chemogenetically activate GC GLP-1R+ neurons, Glp1r-Cre animals received intraperitoneal injections of either sterile saline (vehicle) or the designer receptor exclusively activated by designer drugs (DREADD) agonist JHU37160 dihydrochloride (Bonaventura et al., 2019; J60, 0.1 mg/kg; catalog #HB6261, Hello Bio) 15 min before dark onset in a counterbalanced fashion. To identify potential off-target effects of J60 on feeding behavior, the same behavioral experiment was conducted in two separate cohorts of Glp1r-Cre mice that either (1) did not receive a virus (i.e., no-DREADDs control) or (2) expressed AAV-DIO-eYFP.

To pharmacologically activate GC GLP-Rs, mice received intra-GC infusions 30 min to 1 h before dark-cycle onset. Internal cannulae (extending +3.25 mm beyond pedestal; catalog #C315IMN, P1 Technologies) bilaterally delivered sterile saline (catalog #07-892-4348, Patterson Veterinary) or Ex-4 in 0.25 µl volume. Preweighed food was returned to cages immediately before dark-cycle onset, and measured at 1, 2, and 22 h after dark onset. To determine the impact of a chronic high-fat diet on GC GLP-1R function, mice were maintained on a low-fat (LF) diet [10% kilocalories (kcal) from fat; catalog #D12450Ji, Research Diets) or a HF diet (60% kcal from fat; catalog #D12492i, Research Diets). Diets were provided *ad libitum*, and mice in each group were matched for age, weight, and sex. Mice were maintained on their respective diets for 6 weeks before cannulation and onset of behavioral testing. Following surgical recovery from cannulation (see above, Surgical procedures), acute diet switches occurred 1–4 d following initial intake tests on the maintenance diet (with variance because of how days fell before or after weekends), and the mice were subsequently maintained for 3–4 d on the new diet. The 3–4 d duration on the new diet was to allow a sufficient number of days for the tests during drug or vehicle infusions. Behavioral testing followed the same timeline described above.

At the conclusion of the high-fat diet behavioral experiments, during perfusion for brain collection (see above), abdominal adipose tissue was collected and weighed to confirm weight status. These data are reported as visceral fat over body weight.

Histologic verification of cannulae placement and injection accuracy. For histologic confirmation of AAV-driven transgene expression and cannula placement, mice were anesthetized and perfused as described above. Brains were removed and postfixed for 24 h at 4°C in 30% sucrose in 10% buffered formalin. Coronal sections (40 μM) were collected through the GC. Sections were slide mounted with DAPI Fluoromount-G. Sections displaying AAV-driven transgene expression or cannula tracts were imaged using an upright epifluorescent microscope (Nikon ECLIPSE Ti2e). All mice receiving AAV injections were verified to have region-specific expression in the GC. Six mice with indwelling cannulae implants were excluded from data analysis because of the cannulae being off target. This left a total of 45 cannulated c57bl/6j mice for analyses.

Statistical analysis. We used a between-subjects design for fluorescent *in situ* hybridization, immunohistochemical, electrophysiological, and behavioral experiments examining the effects of maintenance diet (LF or HF) on body weight change. For all other behavioral experiments, within-subjects design was used. Statistical tests included unpaired two-tailed *t* test; paired two-tailed *t* test; paired one-tailed *t* test; one-, two-, or three-way ANOVA; repeated-measures ANOVA (rmANOVA); and multiple comparisons *post hoc* analyses when appropriate (Šidák, Dunnett's, or Greenhouse–Geisser correction) as described in the text. Relationships between cannula placement and behavioral outcomes were assessed with a Pearson's *r* test. Electrophysiological data were tested for normality with the Kolmogorov–Smirnov test. To examine food intake in both male and female mice, the results are presented as chow intake (kcal) divided by body weight (grams) to yield a reflection of food intake corrected by size of the animal. Data are expressed as mean + SEM. Differences in means were considered significant when $p < 0.05$. Statistical tests were performed using GraphPad version 9.2 software.

Results

GLP-1Rs are expressed on neurons within the GC

We used RNAscope to detect *Glp1r* mRNA expression within the GC in C57BL/6J mice. *Glp1r* mRNA was scattered throughout the GC (Fig. 1*A*,*B*,*C*). We quantified the percentage of DAPI-expressing cells that also expressed *Glp1r* mRNA to determine expression levels, which revealed that ~6% of GC cells express *Glp1r* (Fig. 1*D*,*E*). To put this level of GC *Glp1r* mRNA expression in context with other brain regions known to express GLP-1Rs, we quantified *Glp1r* mRNA from the NAc in the same brain sections as those sampled from the GC. NAc neurons are known to express GLP-1Rs, and antagonism of GLP-1Rs in the NAc influences food intake (Dossat et al., 2011; Alhadeff et al., 2012). *Glp1r* mRNA expression in the GC was comparable to that in the NAc ($t_{(8)} = 2.179$, $p = 0.061$, Fig. 1*E*; $n = 4$–5 mice, 2–12 sections averaged/mouse).

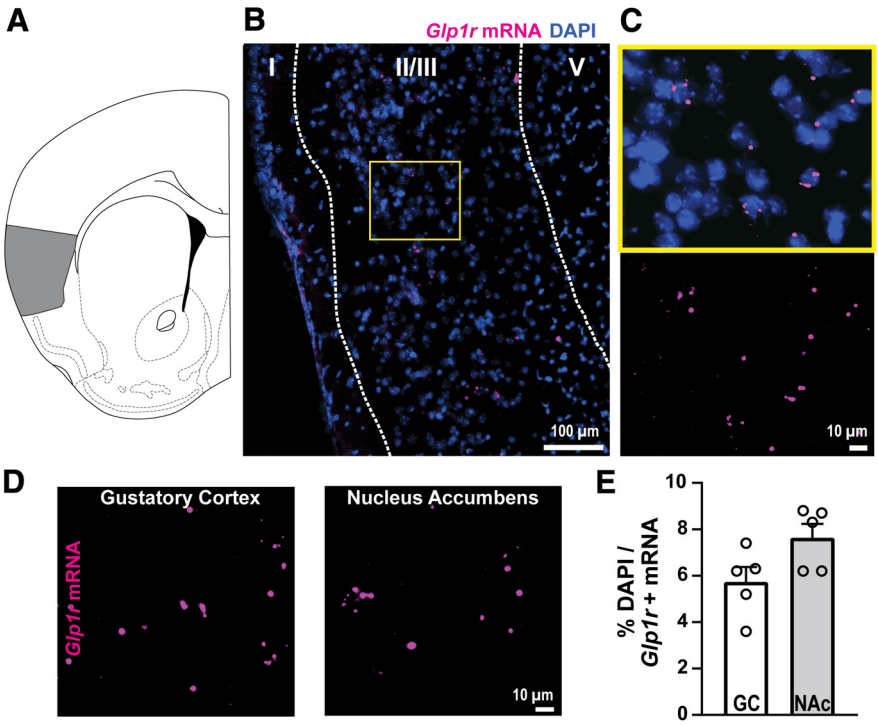

Figure 1. *Glp-1r* mRNA expressed within the GC. ***A***, Localization of the GC (shaded gray) in a coronal section of the mouse brain. ***B***, Representative image of G*lp1r* mRNA and DAPI in GC layer II/III. ***C***, View of yellow-indicated region in ***B*** with (top) and without (bottom) DAPI to aid in visualization of G*lp1r* expression. ***D***, View of G*lp1r* mRNA in the GC and in the NAc from the same coronal section. ***E***, Quantification of *Glp1r* mRNA for each region; $n = 5$ mice, 2–12 sections per mouse.

Next, we paired immunohistochemistry and genetically driven fluorophores in Glp1-Cre mice crossed with the Ai9 tdTomato reporter line (Glp1r-Cre;Ai9) to determine whether there is layer specificity of GC GLP-1Rs and, separately, if they are neuronally localized. Sections from Glp1r-Cre;Ai9 mice revealed significantly higher expression of GLP-1R+ neurons (tdTomato+) within GC layers II/III versus layers V/VI ($t_{(10)} = 9.072$, $p < 0.0001$, Fig. 2*A*,*B*) and higher expression of NeuN+ and GLP-1R+ cells in layers II/III versus layers V/VI (Fig. 2*B*; ($t_{(8)} = 8.507$, $p < 0.0001$). Of the NeuN+ cells within layers II/III, we found that ~5% also expressed GLP-1R (tdTomato+; Fig. 2*C*), a number comparable to that revealed in our prior RNAscope experiment (Fig. 1*E*). Within layers V/VI, ~2% of NeuN+ cells also expressed GLP-1R (Fig. 2*C*). We inspected one mouse throughout the anterior–posterior axis of the insular cortex to find, qualitatively, that roughly similar numbers of tdTomato+ cells are found throughout the insula, perhaps with an increase in the most posterior extent (Fig. 2*D*,*E*). Together, these data indicate the GC GLP-1Rs are localized to neurons and that GLP-1R neurons are more abundant in the dense cell layers II and III of the GC.

GC GLP-1R+ neurons are depolarized by the selective GLP1-R agonist exendin-4

To determine whether activation of GLP-1Rs functionally modulates GC neurons, we performed whole-cell voltage-clamp recordings from layer II/III GC GLP-1R+ and GLP-1RØ neurons visualized in brain slices from Glp1r-Cre;Ai9 mice (Fig. 3*A*). Application of the selective GLP-1R agonist Ex-4 (100 nM) produced an inward current in GLP-1R+ neurons of 16.4 ± 3.2 pA (Ex-4 holding current versus baseline, paired two-tailed *t* test ($t_{(8)} = 5.122$, $p = 0.0009$), but not in neighboring GLP-1RØ neurons (Ex-4 holding current vs baseline in GLP-1RØ neurons, paired two-tailed *t* test, $t_{(8)} = 1.936$, $p = 0.089$; Ex-4-mediated current in GLP-1R+ vs GLP-1RØ neurons, two-tailed Mann–Whitney test, $p = 0.0008$; Fig. 3*B*,*C*). The Ex-4-mediated currents in GLP-1R+ neurons reversed at −85 ± 3.2 mV, which is near the expected reversal potential for potassium, and was associated with an increase in membrane resistance (baseline = 103 ± 12 MΩ vs Ex-4 = 121 ± 14 MΩ, paired two-tailed *t* test, ($t_{(8)} = 5.187$, $p = 0.0008$), indicating a closure of ion channels. In GLP-1RØ neurons there was no effect of Ex-4 on membrane resistance (baseline = 198 ± 41 MΩ vs Ex-4 = 206 ± 41 MΩ, paired two-tailed *t* test, ($t_{(7)} = 0.9111$, $p = 0.393$), consistent with the lack of Ex-4-mediated current in these neurons.

Additionally, GLP-1R+ and GLP-1RØ neurons exhibited different intrinsic properties. GLP1-R+ neurons had a higher membrane capacitance (unpaired two-tailed, *t* test, $t_{(17)} = 2.284$, $p = 0.036$), lower membrane resistance ($t_{(16)} = 2.778$, $p = 0.013$), and more hyperpolarized resting membrane potential ($t_{(17)} = 2.384$, $p = 0.03$) compared with neighboring GC GLP-1RØ neurons (Fig. 3*E*,*F*,*G*). Under current-clamp conditions, the number of action potentials (APs) produced by depolarizing currents was less in GLP-1R+ neurons compared with GLP-1RØ neurons (two-way ANOVA, $F_{(1,13)} = 5.95$, $p = 0.029$; Fig. 3*D*). These data suggest that GLP-1R+ and GLP-1RØ neurons are functionally different populations of neurons and, most important, that GLP-1R+ neurons are depolarized by GLP-1R agonism.

GC GLP-1R+ neurons and GC GLP-1Rs influence food intake

Having identified GLP-1Rs in the GC, and having found that these receptors are functional on the neurons (capable of driving depolarization upon their agonism), we next sought to perform two separate studies to examine the possible causal influence of GC GLP-1Rs on food intake. These included both chemogenetic

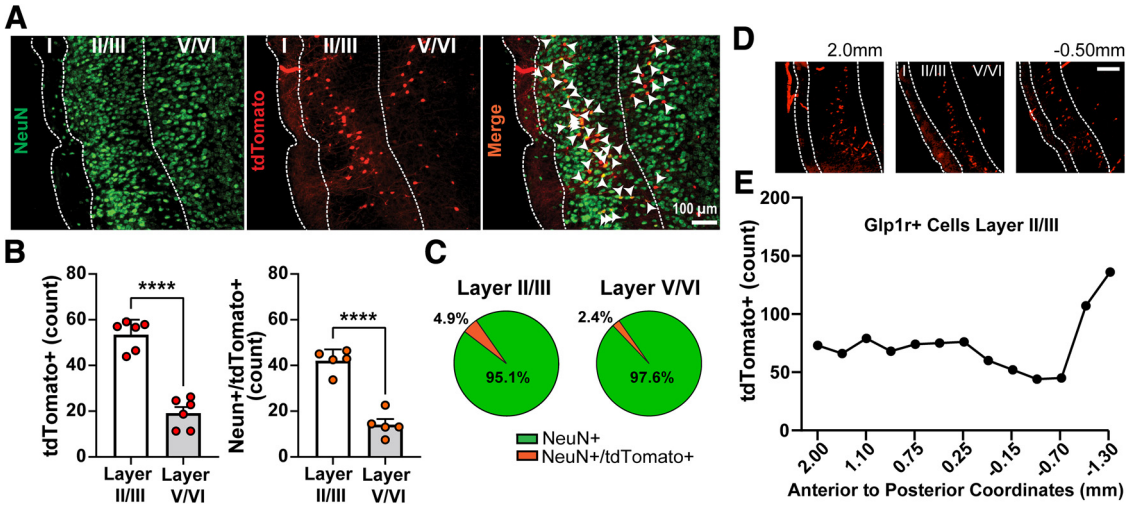

Figure 2. GLP-1Rs are neuronally expressed within the GC. ***A***, Representative image of the GC from a Glp1r-Cre;Ai9 mouse immunolabeled for the neuronal marker NeuN and a merged image showing tdTomato+ somatic colocalization with NeuN (white arrowheads). ***B***, Quantification of tdTomato+ neurons and NeuN+/tdTomato+ neurons in the GC; ****$p < 0.0001$ layer II/III versus V/VI. ***C***, Pie charts depicting percentage of NeuN-expressing and NeuN+/tdTomato+-coexpressing cells within layers II/III and V/VI. Data in ***B*** are mean + SEM. Data in ***B*** and ***C*** are from $n = 6$ mice, 5–10 sections per mouse. ***D***, Representative images of tdTomato+-expressing cells throughout the anterior–posterior axis of the insula cortex. Coordinates are relative to bregma. Scale bar, 100 µm. ***E***, tdTomato+ cell count throughout the anterior–posterior axis of insula cortex layer II/III from the same mouse as in ***D***.

manipulation of GC GLP-1R+ neurons, and pharmacological interrogation of the GC GLP-1Rs. In both studies, we examined dark-cycle intake of standard chow/food pellets as a simple assay for homeostatic food intake.

In the first experiment, we chemogenetically activated GC GLP-1R+ neurons via administration of the DREADD ligand J60 (0.1 mg/kg, i.p.) in Glp1r-Cre mice with bilateral expression of AAV-DIO-hM3D(Gq) in the GC (Fig. 4*A*,*B*). Following several weeks to allow DREADD expression, mice were acclimated and tested for dark-cycle intake of chow (Fig. 4*C*; see above, Materials and Methods). There was no significant effect of sex (two-way ANOVA, sex, $F_{(1,5)} = 0.089$, $p = 0.778$; DREADD agonism, $F_{(1,5)} = 3.93$, $p = 0.104$) as such data were pooled across sexes. Chemogenetic activation of GC GLP-1R+ neurons significantly reduced chow intake at 1 h after dark onset (one-tailed, paired *t* test, $t_{(6)} = 2.066$, $p = 0.042$, Fig. 4*D*, left), with no effect at 2 or 24 h (data not shown). Importantly, a separate group of Glp1r-Cre mice that did not express AAV revealed that J60 at the same dose as above did not influence chow intake (one-tailed, paired *t* test, $t_{(6)} = 0.416$, $p = 0.346$, Fig. 4*D*, right). A third group of Glp1r-Cre mice injected into the GC with AAV-DIO-eYFP as a control virus similarly supports no influence of systemic J60 (same dose) on chow intake (one-tailed, paired *t* test, $t_{(4)} = 0.277$, $p = 0.398$; data not shown); together indicating the effect of J60 on food intake is specific to DREADD receptor activation.

In the second experiment, we delivered the GLP-1R agonist Ex-4 at a range of doses in a counterbalanced order over different days into the GC of C57BL/6J mice via bilateral indwelling cannulae. Based on our anatomic data (Fig. 2*B*), we attempted to target GLP-1Rs within GC layers II/III because of the high numbers of GLP-1R+ neurons in these layers. There was no significant effect of sex (two-way ANOVA, sex, $F_{(1,8)} = 0.562$, $p = 0.475$; Ex-4, $F_{(2.748,21.99)} = 5.392$, $p = 0.007$), and therefore going forward, the data were pooled across sexes. We found that intra-GC Ex-4 significantly reduced dark-cycle chow intake at 2 h after dark onset (one-way ANOVA, $F_{(2.718,24.46)} = 5.693$, $p = 0.005$). Significant reductions in chow intake were uncovered following infusions of both 0.03 and 0.1 µg of Ex-4 (Dunnett's *post hoc*, $t_{(9)} = 3.067$, $p = 0.034$; $t_{(9)} = 3.72$, $p = 0.012$, respectively; Fig. 5*B*). There was no significant correlation between the anterior–posterior location of the Ex-4 infusion and the magnitude of chow intake suppression 2 h after dark onset (Pearson's *r*, $r_{(10)}$ 0.616, $p = 0.058$ and $r_{(10)}$ 0.359, $p = 0.309$; 0.1 µg and 0.03 µg of Ex-4, respectively). Together, the results of both the chemogenetic and pharmacological experiments support a role for GC GLP-1Rs in influencing homeostatic food intake.

Effect of GC GLP-1R agonism on palatable food intake

Although homeostatic food intake reflects a basic desire to consume food, ingestive behavior is a complex process mediated by a variety of both internal and external factors. Therefore, we next explored whether the above effects of GC GLP-1Rs on food intake extended into influencing the consumption of palatable foods and if this may be also modulated by the metabolic state of the mice. To accomplish this, C57BL/6J mice were given *ad libitum* access to either LF (10% kcal fat) or HF (60% kcal fat) diet for 6 weeks or not in the HF or LF groups, respectively. Consistent with prior reports, we observed an increase in body weight in HF-maintained animals soon on diet onset (Williams et al., 2011; Honors et al., 2012; Salinero et al., 2018; Maric et al., 2022). There was a significant main effect of diet, time on diet, and an interaction between diet multiplied by time on change in body weight (two-way ANOVA, diet, $F_{(1,33)} = 30.06$, $p < 0.0001$; time, $F_{(1.751,57.80)} = 66.73$, $p < 0.0001$; interaction, $F_{(5,165)} = 26.99$, $p < 0.0001$; Fig. 6*A*). Also as expected (Hwang et al., 2010; Carlin et al., 2016; Salinero et al., 2018; Maric et al., 2022), we observed a sex difference in body weight gains, wherein females exhibited less weight gain compared with males when maintained on the same HF diet (Fig. 6*B*). This was confirmed via fat pad analysis at the conclusion of the experiment (Fig. 6*G*). We compared changes in body weight of males and females over the 6 weeks of HF consumption and identified a significant main effect of sex (two-way ANOVA, $F_{(1,20)} = 7.111$, $p = 0.0148$), a significant effect of time on diet ($F_{(1.598,31.95)} = 70.24$, $p < 0.0001$), and a significant interaction between sex multiplied by time on diet ($F_{(5,100)} = 4.99$, $p = 0.0004$). An examination of the body weight change in HF males and females only at week 6 revealed a significant effect

of sex (two-tailed, unpaired t test, $t_{(20)} = 4.023$, $p = 0.0007$; Fig. 6*C*).

After 6 weeks on the respective diets, and having confirmed a gain in body weight because of chronic high-fat diet (as above), the GC was cannulated, and mice received intra-GC Ex-4 following the same treatment timeline as above. There was no effect of sex (two-way ANOVA, sex, $F_{(1,20)} = 1.483$, $p = 0.238$), so data are pooled across males and females. The HF group consuming the HF diet exhibited no Ex-4-induced reductions in food intake at 2 h into the dark cycle (rmANOVA, $F_{(1.404,28.08)} = 2.199$, $p = 0.142$; Fig. 6*D*, left). After an acute diet switch (see above, Materials and Methods; Fig. 6*E*), we examined intra-GC Ex-4-induced responses in the HF group consuming an LF diet. Again there was no effect of sex (two-way ANOVA, sex, $F_{(1,20)} = 0.200$, $p = 0.659$), so the data were pooled. In mice that were on the chronic HF diet, there was a significant main effect of Ex-4 to reduce LF diet intake at 2 h into the dark cycle (rmANOVA, $F_{(2,21)} = 9.801$, $p = 0.001$; Fig. 6*F*). *Post hoc* tests revealed significant effects of both 0.1 and 0.3 µg Ex-4 ($t_{(21)} = 2.519$, $p = 0.037$; $t_{(21)} = 4.307$, $p = 0.001$; respectively). Likewise, in mice that were on the LF diet, there was a significant main effect of Ex-4 to reduce HF diet intake at 2 h into the dark cycle (rmANOVA, $F_{(2,12)} = 3.96$, $p = 0.042$; Fig. 6*F*). *Post hoc* tests revealed a significant effect of 0.3 µg Ex-4 ($t_{(12)} = 2.520$, $p = 0.049$). The LF group consuming the LF diet exhibited no Ex-4-induced reductions in food intake at 2 h into the dark cycle (rmANOVA, $F_{(2,12)} = 0.733$, $p = 0.478$; Fig. 6*D*, right). Postmortem analyses confirmed that the mice contributing to these data had cannulae localized within the GC (Fig. 6*H*). Together with the influence of GC GLP-1Rs in modulating intake of standard lab chow (Fig. 5), these results suggest that GC GLP-1Rs may influence both homeostatic (eating standard lab chow) and hedonic (preferring HF or LF) food intake.

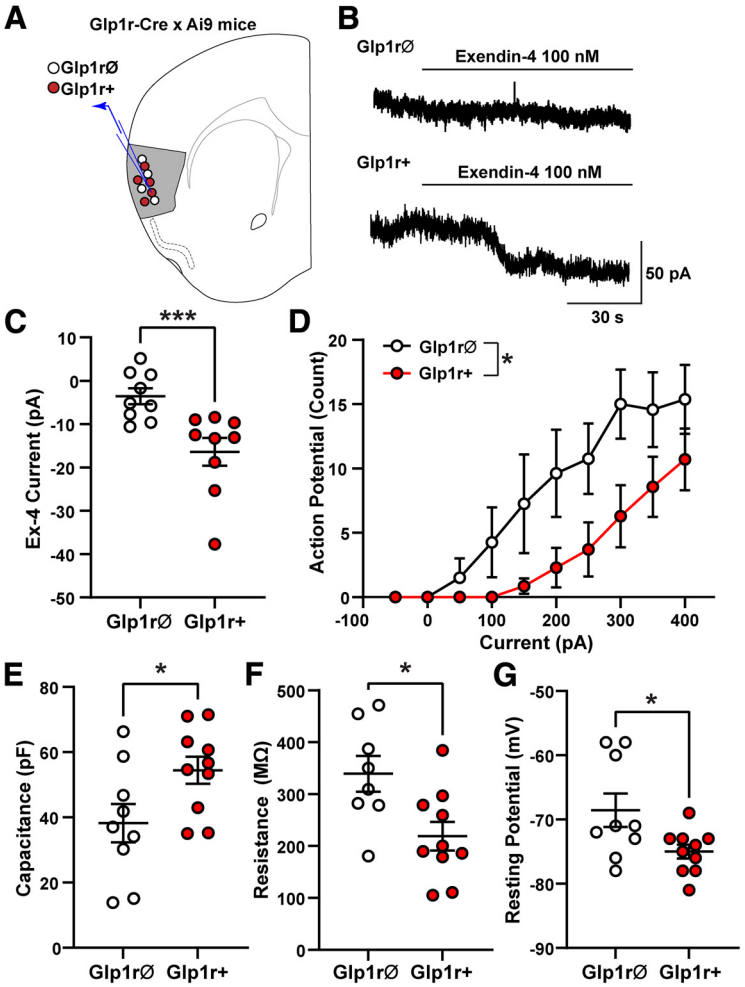

Figure 3. GC GLP1-R+ neurons are depolarized by Ex-4 and exhibit distinct electrophysiological properties versus neighboring GLP-1RØ neurons. ***A***, Whole-cell voltage-clamp recordings were made from GC layer II/III GLP-1R+ and GLP-1RØ neurons from Glp1r-Cre;Ai9 mice ($n = 9$ mice, 6 male, 3 female; 1–4 neurons/mouse). ***B***, Example recording from GLP-1RØ neuron showing no Ex-4-mediated current (top trace) and an example recording from GLP-1R+ neuron showing slow inward current induced by bath application of Ex-4 (100 nM; bottom trace). ***C***, Ex-4-mediated inward currents were larger in GLP-1R+ neurons compared with GLP-1RØ neurons; $^{***}p = 0.0008$, two-tailed Mann–Whitney test. ***D***, Number of action potentials elicited with increasing current steps was different in GLP-1R+ and GLP-1RØ neurons (two-way ANOVA, $F_{(1,13)} = 5.95$, $p = 0.0298$). ***E–G***, GLP-1R+ and GLP-1RØ neurons had different intrinsic properties, including capacitance (***E***), membrane resistance (***F***), and resting membrane potential (***G***). Data are mean ± SEM, $n = 7$–10/group; $^{*}p < 0.05$ by unpaired t test.

Discussion

The GC integrates taste, valence, and interoceptive information. Cells within the GC are well known to exhibit tastant-evoked responses relating to tastant identity as well as the palatability of tastants (Katz et al., 2001; Small et al., 2003; Stapleton et al., 2006; Jezzini et al., 2013; Maier and Katz, 2013; Fletcher et al., 2017; Chen et al., 2021). Yet, it is interesting to note that some GC cells do not respond to tastants, and there are both layer and cell-type-specific responses within the GC (Dikecligil et al., 2020). This heterogeneity within the GC underscores the need for understanding the role of distinct neuronal populations within this brain area that may contribute to behavior, especially ingestive behaviors. Indeed, in addition to taste processing, GC activity is modulated by the prandial state, wherein activity is highest when hungry and reduced when satiated (Small et al., 2001; Saper, 2002; Hinton et al., 2004; de Araujo et al., 2006; Van Bloemendaal et al., 2014). Additionally, preclincial work demonstrated that GC neurons are sensitive to the metabolic state (i.e., fasted or fed) and respond to food-predicting cues more robustly when fasted versus fed (Livneh et al., 2017, 2020). The insular cortex is a major component of the enteroinsular axis, and GLP-1 is a potent modulator of this axis (Creutzfeldt, 2001). In the present study, we demonstrate the presence and functionality of GLP-1Rs within the GC.

Localization of functional GLP-1Rs in the GC

To our knowledge, we provide the first evidence for GLP-1R expression within the GC. We found that ~5% of GC cells express *Glp1r* mRNA, a finding corroborated when crossing Glp1r-Cre mice with Ai9 Tdtomato reporter mice. Although this is a relatively small proportion of cells, we found this expression level was comparable to that in the NAc, a region in which GLP-1R agonism reduces food intake (Dossat et al., 2011, 2013; Alhadeff et al., 2012). Prior work in a different brain region uncovered evidence for expression of GLP-1Rs on astrocytes (Reiner et al., 2016). Importantly, through

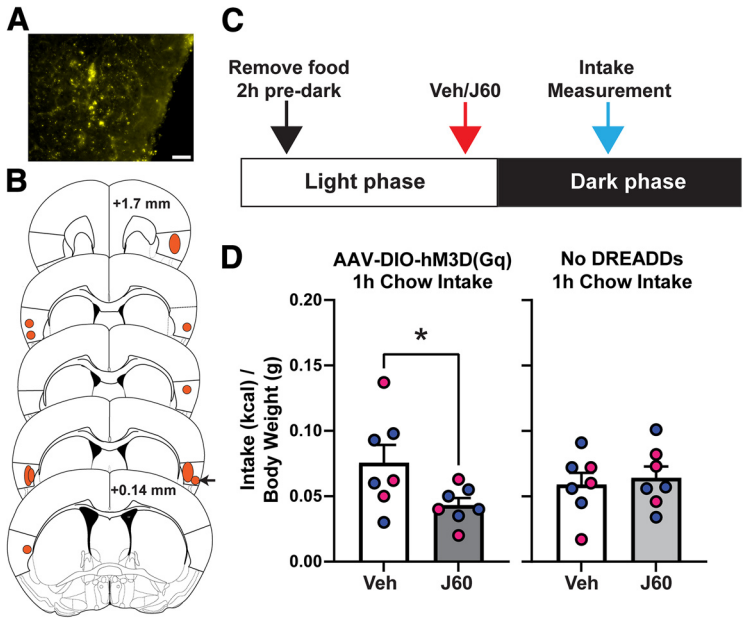

Figure 4. Chemogenetic activation of GC GLP-1R+ neurons reduces dark-cycle chow intake. ***A***, Example image of DREADD expression (YFP+) in the GC from one mouse. Scale bar, 50 µm. ***B***, Shaded regions illustrating representative spread of AAV-DIO-hM3D(Gq)-mCitrine expression within the GC. Anterior–posterior (AP) coordinates are relative to bregma. Arrow indicates example mouse shown in ***A***. ***C***, Schematic of experimental timeline. ***D***, Effect of DREADD ligand J60 (0.1 mg/kg, i.p.) on dark-cycle chow intake in Glp1r-Cre mice bilaterally expressing GC AAV-DIO-hM3D(Gq)-mCitrine, and in Glp1r-Cre mice that do not express DREADD receptors. Mean + SEM of chow consumed (corrected to kcal consumed divided by body weight); $n = 7$/group, 3 females, 4 males (blue circles, males; pink circles, female; $^*p < 0.05$ vs vehicle).

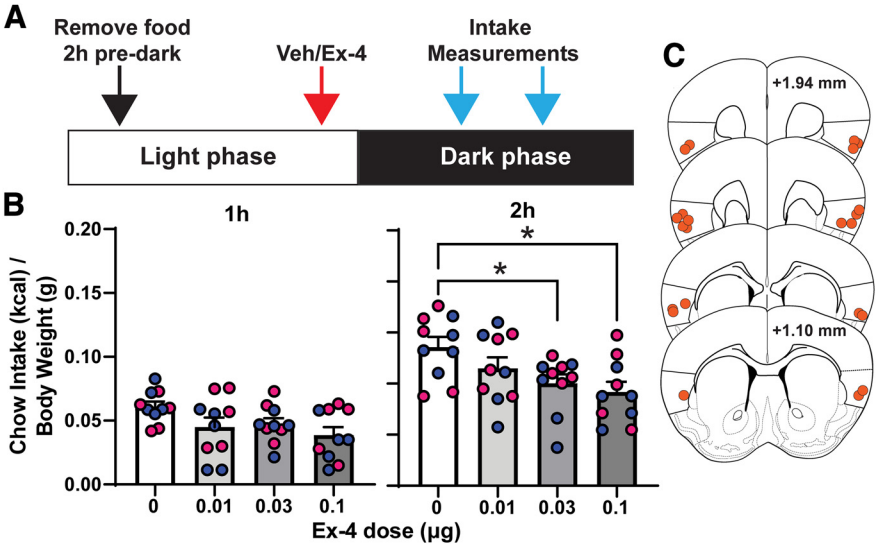

Figure 5. Pharmacological activation of GC GLP-1Rs reduced dark-cycle chow intake. ***A***, Schematic of experimental timeline. ***B***, Effect of intra-GC Ex-4 on chow intake at 1 and 2 h into the dark cycle. ***B***, Mean + SEM of chow consumed (corrected to kcal consumed divided by body weight); $n = 10$/group, 5/sex; blue circles, males; pink circles, female; $^*p < 0.05$ versus vehicle. ***C***, Representative cannula placements. Anterior–posterior (AP) coordinates are relative to bregma.

immunohistochemistry with the neuronal marker NeuN in Glp1r-Cre;Ai9 mice, we verified that GLP-1R+ cells in the GC appear to be neurons, consistent with the majority of research in other brain regions (Tauchi et al., 2008; Richard et al., 2014; Fortin et al., 2020; Zeng et al., 2021). What transmitters GLP-1R+ neurons synthesize/release will be important to address.

The differing GC layers subserve distinct roles in sensory processing. For instance, layers V/VI contain a large number of taste-sensitive neurons (Kayyal et al., 2019; Dikecligil et al., 2020). More GLP-1R+ neurons were found within layers II/III of the GC, with GLP-1R+ neurons detected within layers V/VI but at a significantly lower level than layers II/III. Although the synaptic organization of the GC is a topic of much interest (Haley et al., 2016, 2020), it has received considerably less attention than the synaptic organization of many other cortices. Future research will be needed to define the synaptic/circuit contributions of GLP-1R signaling on GC neurons, especially concerning if and how signaling via layers II/III GC neurons may possibly influence taste processing among the more deep taste-responsive neurons found in layers V/VI.

Perhaps informing the above goal to some extent, we found that application of Ex-4 produced a slow inward current in GLP-1R+ neurons, which was similar in amplitude to inward currents produced by GLP-1 in other areas of the brain (Cork et al., 2015). However, GLP-1Rs may depolarize GC neurons using different intracellular mechanisms and ion channels as currents in GC neurons reversed near the potassium equilibrium potential and were associated with a decrease in conductance (indicating closing of potassium channels), whereas GLP-1R-mediated currents in the paraventricular nucleus, bed nucleus of the stria terminalis, and hippocampus were associated with an increase in conductance. In addition, GLP-1R+ neurons had different intrinsic properties compared with neighboring GLP-1RØ neurons, suggesting that although GLP-1R+ neurons are localized to the densely packed layers II/III of the GC, they represent a unique population of neurons within the GC. An alternative interpretation is that differences in intrinsic properties between GLP-1R+ and GLP-1RØ neurons may be attributable to tdTomato expression in GLP-1R+ neurons. Although we cannot conclusively rule out this possibility, it is worth noting that tdTomato expression does not affect the intrinsic properties of other neuron types, including principal neurons in the prefrontal cortex (Anastasiades et al., 2019) and striatum (Ade et al., 2011), and interneurons in the somatosensory cortex, hippocampus, and striatum (Kaiser et al., 2016).

A role for GC GLP-1Rs in ingestive behavior

The GLP-1 system is implicated in processing sensory cues, including odors (Thiebaud et al., 2016), in manners important for food intake. To examine the functional role of GC GLP-1R+ neurons in food intake, and, separately, GLP-1R signaling within GC neurons, we used both chemogenetics and pharmacology in

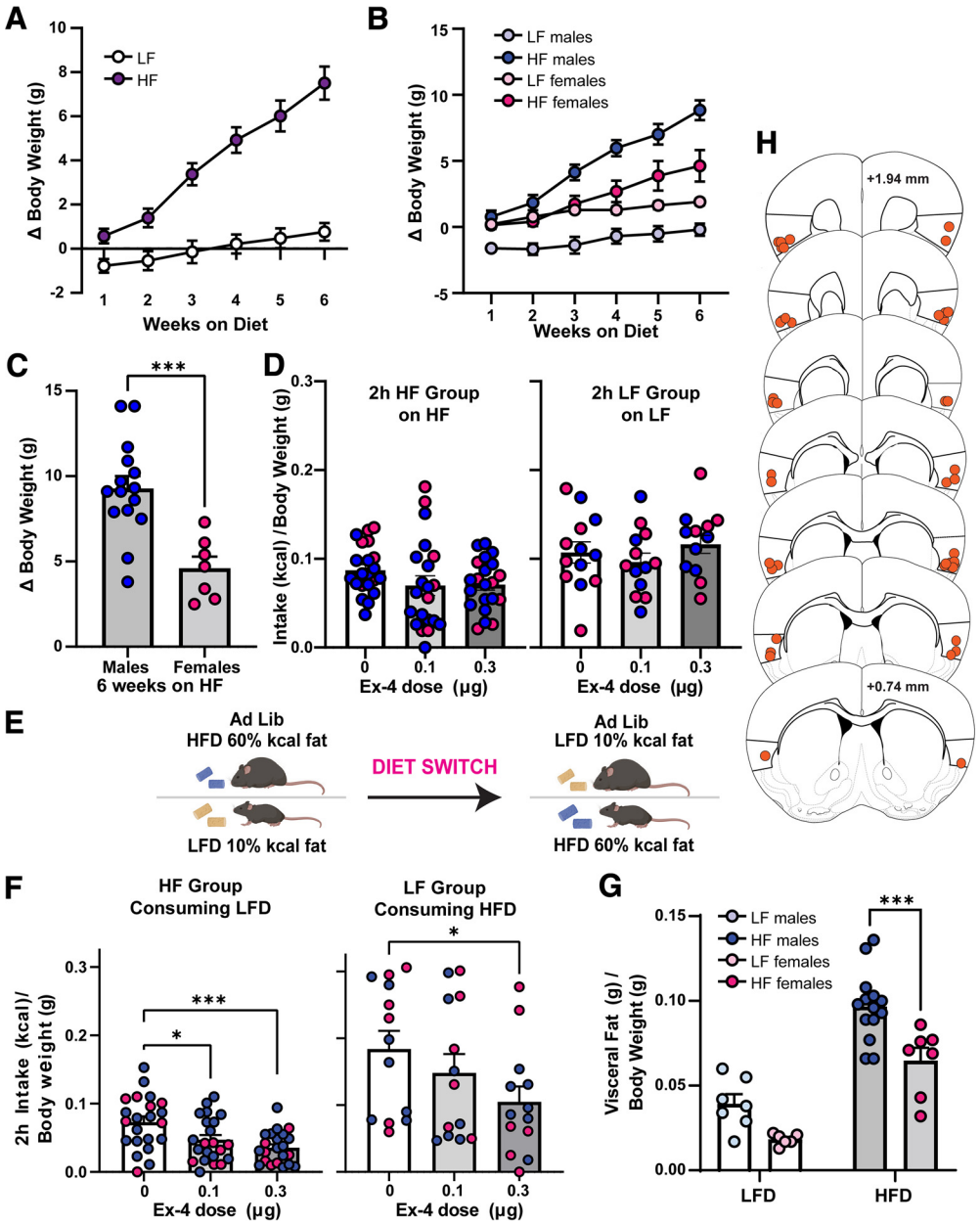

Figure 6. Impact of intra-GC Ex-4 in context of a chronic high-fat diet. ***A***, Weekly elevations in body weight of mice on the LF or HF diet during the development of weight gain over 6 weeks. ***B***, Weekly elevations in body weight from ***A***, divided by sex. ***C***, Comparing the average change in body weight on the sixth week of HF maintenance in males and females; ***$p <$ 0.001 males versus females. ***D***, Intake (kcal/body weight) of HF by the HF-maintained group, 2 h into the dark cycle following intra-GC Ex-4 (left) or the same when LF group was monitored for LF intake (right). ***E***, Schematic of experimental timeline, cohort of animals on HF acutely switched to LF (top), or cohort of animals on LF acutely switched to HF (bottom). ***F***, Left, LF food intake (kcal/body weight) of the HF-maintained group, 2 h into the dark cycle following intra-CG Ex-4 infusion; *$p < 0.05$, ***$p < 0.001$ versus 0 µg Ex-4. Right, HF food intake (kcal/body weight) of the LF-maintained group, 2 h into the dark cycle following intra-GC Ex-4; *$p < 0.05$ 0.3 versus 0 µg Ex-4. ***G***, Visceral fat (g) calculated over body weight (g) at the end of the experiment (see above, Materials and Methods); ***$p < 0.005$ HF males versus HF females. ***H***, Representative cannula infusion tip placements of mice included in ***D***, ***F***, and ***G***; n = 13–22 mice/diet condition.

separate groups of mice. First, we used chemogenetic targeting of GLP-1R+ neurons using Glp1r-Cre mice expressing excitatory DREADD in their GC. When GC GLP-1R+ neurons were activated just before the onset of the dark cycle, chow intake was significantly reduced as compared with the control condition. This indicates that this cell population influences ingestive behavior. These results are in agreement with recent work from several groups supporting roles for subsets, sometimes sparse subsets, of GC neurons (e.g., PKC-δ+, Nos1+, CaMKIIα+) to influence ingestive behavior (Stern et al., 2020, 2021; Wu et al., 2020; Zhang-Molina et al., 2020).

We followed up our chemogenetic findings by exploring how pharmacological manipulation of specifically the receptors themselves would influence homeostatic feeding. We found that activation of GC GLP-1Rs with Ex-4 significantly reduced dark-cycle chow intake. This was achieved within a dose range that has been reported for other brain regions (Swick et al., 2015; Ong et al., 2017; López-Ferreras et al., 2018; Reiner et al., 2018). These data indicate that GLP-1R signaling on GC neurons contributes to the control of homeostatic food intake, consistent with work in other brain areas (Tang-Christensen et al., 1996; Dossat et al., 2011; Kanoski et al., 2011; Hsu et al., 2015; Terrill et

al., 2019). We observed similar outcomes in males and females to intra-GC GLP-1R activation, which is consistent with prior research on the lateral ventricle (Richard et al., 2016) but inconsistent with effects within the lateral hypothalamus that did uncover sex differences (López-Ferreras et al., 2019). These distinct effects are likely mediated by the brain region targeted because activation of GLP-1Rs can yield differing effects depending on brain region (for review, see Williams, 2022).

Pathophysiological states, like those associated with higher body weights, have an impact on GC activity. Specifically, the GC of obese individuals displays greater activation in response to taste stimuli and food-associated cues than nonobese individuals (Van Bloemendaal et al., 2014; Avery et al., 2017; Bohon, 2017; Li et al., 2017). The GLP-1 system itself is also affected by obesity. Maintenance on a high fat diet reduces GLP-1R expression in a brain-region-specific manner (Mul et al., 2013) and impairs anorexigenic effects of peripherally administered GLP-1R agonists (Williams et al., 2011; Duca et al., 2013; Mul et al., 2013; Mella et al., 2017). In the present study, we aimed to determine the effect of a chronic high-fat diet on the effects of GC GLP-1Rs on food intake. Male and female mice were maintained on a LF diet or a HF diet for 6 weeks to induce the chronic high-fat diet phenotype in the latter group. We found that mice maintained on either diet were insensitive to the effects of GC GLP-1R activation. However, following acute switches, mice in both the HF and LF chronic groups exhibited significant reductions in food intake to their alternative/new diet following GC GLP-1R activation. Together, these data suggest that GC GLP-1Rs remain functional in chronic high-fat diet conditions, yet palatability may have an impact on the ability of GC GLP-1R agonism to reduce intake. It is important to note that we did not examine expression levels of GLP-1Rs in these chronic diet conditions. Future investigations examining the impact of diet on GLP-1R expression in the GC, and its functionality, will be important.

Conclusion

The present study demonstrates that a population of GC neurons express GLP-1Rs, these neurons are depolarized by agonism of GLP-1R, and these receptors can influence food intake upon their activation, including in manners depending on the metabolic state of the animal and food hedonic value. This work provides a foundation for future work to resolve the upstream (Where does GLP-1 arise from to reach the GC?) and downstream circuitry for the GC GLP-1R system (Where do GC GLP-1R+ neurons innervate to influence behavior?). It would be of interest to investigate a possible role for GC GLP-1Rs in the known effects of GLP-1 mimetics in managing obesity (Wilding et al., 2021). Further, given the extensive connectivity of the insular cortex, it is important to note that the GC GLP-1R system may have implications beyond ingestive behavior and metabolic conditions. Indeed, awareness for a potential modulatory role of GLP-1 mimetics in a variety of human conditions is increasing (Brauer et al., 2020).

References

Accolla R, Carleton A (2008) Internal body state influences topographical plasticity of sensory representations in the rat gustatory cortex. Proc Natl Acad Sci U S A 105:4010–4015.

Ade KK, Wan Y, Chen M, Gloss B, Calakos N (2011) An improved BAC transgenic fluorescent reporter line for sensitive and specific identification of striatonigral medium spiny neurons. Front Syst Neurosci 5:32.

Alhadeff AL, Rupprecht LE, Hayes MR (2012) GLP-1 neurons in the nucleus of the solitary tract project directly to the ventral tegmental area and nucleus accumbens to control for food intake. Endocrinology 153:647–658.

Anastasiades PG, Boada C, Carter AG (2019) Cell-type-specific D1 dopamine receptor modulation of projection neurons and interneurons in the prefrontal cortex. Cereb Cortex 29:3224–3242.

Armbruster BN, Li X, Pausch MH, Herlitze S, Roth BL (2007) Evolving the lock to fit the key to create a family of G protein-coupled receptors potently activated by an inert ligand. Proc Natl Acad Sci U S A 104:5163–5168.

Avery JA, Powell JN, Breslin FJ, Lepping RJ, Martin LE, Patrician TM, Donnelly JE, Savage CR, Simmons WK (2017) Obesity is associated with altered mid-insula functional connectivity to limbic regions underlying appetitive responses to foods. J Psychopharmacol 31:1475–1484.

Baldo BA, Spencer RC, Sadeghian K, Mena JD (2016) GABA-mediated inactivation of medial prefrontal and agranular insular cortex in the rat: contrasting effects on hunger- and palatability-driven feeding. Neuropsychopharmacol 41: 960–970.

Bohon C (2017) Brain response to taste in overweight children: a pilot feasibility study. PLoS One 12:e0172604.

Bonaventura J, et al. (2019) High-potency ligands for DREADD imaging and activation in rodents and monkeys. Nat Commun 10:4627.

Bouaichi CG, Vincis R (2020) Cortical processing of chemosensory and hedonic features of taste in active licking mice. J Neurophysiol 123:1995–2009.

Brauer R, Wei L, Ma T, Athauda D, Girges C, Vijiaratnam N, Auld G, Whittlesea C, Wong I, Foltynie T (2020) Diabetes medications and risk of Parkinson's disease: a cohort study of patients with diabetes. Brain 143:3067–3076.

Carlin JL, McKee SE, Hill-Smith T, Grissom NM, George R, Lucki I, Reyes TM (2016) Removal of high fat diet after chronic exposure drives binge behavior and dopaminergic dysregulation in female mice. Neuroscience 326:170– 179.

Chen K, Kogan JF, Fontanini A (2021) Spatially distributed representation of taste quality in the gustatory insular cortex of behaving mice. Curr Biol 31:247–256.e4.

Cork SC, Richards JE, Holt MK, Gribble FM, Reimann F, Trapp S (2015) Distribution and characterisation of Glucagon-like peptide-1 receptor expressing cells in the mouse brain. Mol Metab 4:718–731.

Crespo CS, Cachero AP, Jiménez LP, Barrios V, Ferreiro EA (2014) Peptides and food intake. Front Endocrinol (Lausanne) 5:58.

Creutzfeldt W (2001) The entero-insular axis in type 2 diabetes—incretins as therapeutic agents. Exp Clin Endocrinol Diabetes 109:S288–S303.

de Araujo IE, Gutierrez R, Oliveira-Maia AJ, Pereira A, Nicolelis MAL, Simon SA (2006) Neural ensemble coding of satiety states. Neuron 51:483–494.

Dickson SL, Shirazi RH, Hansson C, Bergquist F, Nissbrandt H, Skibicka KP (2012) The glucagon-like peptide 1 (GLP-1) analogue, exendin-4, decreases the rewarding value of food: a new role for mesolimbic GLP-1 receptors. J Neurosci 32:4812–4820.

Dikecligil GN, Graham DM, Park IM, Fontanini A (2020) Layer- and cell type-specific response properties of gustatory cortex neurons in awake mice. J Neurosci 40:9676–9691.

Di Lorenzo PM (2021) Neural coding of food is a multisensory, sensorimotor function. Nutrients 13:398–10.

Dossat AM, Lilly N, Kay K, Williams DL (2011) Glucagon-like peptide 1 receptors in nucleus accumbens affect food intake. J Neurosci 31:14453–14457.

Dossat AM, Diaz R, Gallo L, Panagos A, Kay K, Williams DL (2013) Nucleus accumbens GLP-1 receptors influence meal size and palatability. Am J Physiol Endocrinol Metab 304:E1314–E1320.

Duca FA, Sakar Y, Covasa M (2013) Combination of obesity and high-fat feeding diminishes sensitivity to GLP-1R agonist exendin-4. Diabetes 62:2410– 2415.

Fletcher ML, Ogg MC, Lu L, Ogg RJ, Boughter JD (2017) Overlapping representation of primary tastes in a defined region of the gustatory cortex. J Neurosci 37:7595–7605.

Fortin SM, Lipsky RK, Lhamo R, Chen J, Kim E, Borner T, Schmidt HD, Hayes MR (2020) GABA neurons in the nucleus tractus solitarius express GLP-1 receptors and mediate anorectic effects of liraglutide in rats. Sci Transl Med 12:eaay8071.

Gautron L, Elmquist JK, Williams KW (2015) Neural control of energy balance: translating circuits to therapies. Cell 161:133–145.

Gehrlach DA, Weiand C, Gaitanos TN, Cho E, Klein AS, Hennrich AA, Conzelmann K-K, Gogolla N (2020) A whole-brain connectivity map of mouse insular cortex. Elife 9:e55585.

Haley MS, Fontanini A, Maffei A (2016) Laminar- and target-specific amygdalar inputs in rat primary gustatory cortex. J Neurosci 36:2623–2637.

Haley MS, Bruno S, Fontanini A, Maffei A (2020) LTD at amygdalocortical synapses as a novel mechanism for hedonic learning. Elife 9:e55175.

Hinton EC, Parkinson JA, Holland AJ, Arana FS, Roberts AC, Owen AM (2004) Neural contributions to the motivational control of appetite in humans. Eur J Neurosci 20:1411–1418.

Hisadome K, Reimann F, Gribble FM, Trapp S (2010) Leptin directly depolarizes preproglucagon neurons in the nucleus tractus solitarius: electrical properties of glucagon-like peptide 1 neurons. Diabetes 59:1890–1898.

Hisadome K, Reimann F, Gribble FM, Trapp S (2011) CCK stimulation of GLP-1 neurons involves α 1-adrenoceptor-mediated increase in glutamatergic synaptic inputs. Diabetes 60:2701–2709.

Honors MA, Hargrave SL, Kinzig KP (2012) Glucose tolerance in response to a high-fat diet is improved by a high-protein diet. Obesity (Silver Spring) 20:1859–1865.

Hsu TM, Hahn JD, Konanur VR, Lam A, Kanoski SE (2015) Hippocampal GLP-1 receptors influence food intake, meal size, and effort-based responding for food through volume transmission. Neuropsychopharmacology 40:327–337.

Hwang L-L, Wang C-H, Li T-L, Chang S-D, Lin L-C, Chen C-P, Chen C-T, Liang K-C, Ho I-K, Yang W-S, Chiou L-C (2010) Sex differences in high-fat diet-induced obesity, metabolic alterations and learning, and synaptic plasticity deficits in mice. Obesity (Silver Spring) 18:463–469.

Jezzini A, Mazzucato L, La Camera G, Fontanini A (2013) Processing of hedonic and chemosensory features of taste in medial prefrontal and insular networks. J Neurosci 33:18966–18978.

Kaiser T, Ting JT, Monteiro P, Feng G (2016) Transgenic labeling of parvalbumin-expressing neurons with tdTomato. Neuroscience 321:236–245.

Kanoski SE, Fortin SM, Arnold M, Grill HJ, Hayes MR (2011) Peripheral and central GLP-1 receptor populations mediate the anorectic effects of peripherally administered GLP-1 receptor agonists, liraglutide and exendin-4. Endocrinology 152:3103–3112.

Katz DB, Simon SA, Nicolelis MA (2001) Dynamic and multimodal responses of gustatory cortical neurons in awake rats. J Neurosci 21:4478–4489.

Katz DB, Nicolelis MA, Simon SA (2002) Gustatory processing is dynamic and distributed. Curr Opin Neurobiol 12:448–454.

Kayyal H, Yiannakas A, Kolatt Chandran S, Khamaisy M, Sharma V, Rosenblum K (2019) Activity of insula to basolateral amygdala projecting neurons is necessary and sufficient for taste valence representation. J Neurosci 39:9369–9382.

Larsen PJ, Tang-Christensen M, Holst JJ, Orskov C (1997) Distribution of glucagon-like peptide-1 and other preproglucagon-derived peptides in the rat hypothalamus and brainstem. Neuroscience 77:257–270.

Li Q, Jin R, Yu H, Lang H, Cui Y, Xiong S, Sun F, He C, Liu D, Jia H, Chen X, Chen S, Zhu Z (2017) Enhancement of neural salty preference in obesity. Cell Physiol Biochem 43:1987–2000.

Livneh Y, Ramesh RN, Burgess CR, Levandowski KM, Madara JC, Fenselau H, Goldey GJ, Diaz VE, Jikomes N, Resch JM, Lowell BB, Andermann ML (2017) Homeostatic circuits selectively gate food cue responses in insular cortex. Nature 546:611–616.

Livneh Y, Sugden AU, Madara JC, Essner RA, Flores VI, Sugden LA, Resch JM, Lowell BB, Andermann ML (2020) Estimation of current and future physiological states in insular cortex. Neuron 105:1094–1111.e10.

López-Ferreras L, Richard JE, Noble EE, Eerola K, Anderberg RH, Olandersson K, Taing L, Kanoski SE, Hayes MR, Skibicka KP (2018) Lateral hypothalamic GLP-1 receptors are critical for the control of food reinforcement, ingestive behavior and body weight. Mol Psychiatry 23:1157–1168.

López-Ferreras L, Eerola K, Mishra D, Shevchouk OT, Richard JE, Nilsson FH, Hayes MR, Skibicka KP (2019) GLP-1 modulates the supramammillary nucleus-lateral hypothalamic neurocircuit to control ingestive and motivated behavior in a sex divergent manner. Mol Metab 20:178–193.

Madisen L, Zwingman TA, Sunkin SM, Oh SW, Zariwala HA, Gu H, Ng LL, Palmiter RD, Hawrylycz MJ, Jones AR, Lein ES, Zeng H (2010) A robust and high-throughput Cre reporting and characterization system for the whole mouse brain. Nat Neurosci 13:133–140.

Maffei A, Haley M, Fontanini A (2012) Neural processing of gustatory information in insular circuits. Curr Opin Neurobiol 22:709–716.

Maier JX, Katz DB (2013) Neural dynamics in response to binary taste mixtures. J Neurophysiol 109:2108–2117.

Malik S, McGlone F, Bedrossian D, Dagher A (2008) Ghrelin modulates brain activity in areas that control appetitive behavior. Cell Metab 7:400–409.

Maric I, Krieger JP, van der Velden P, Börchers S, Asker M, Vujicic M, Wernstedt Asterholm I, Skibicka KP (2022) Sex and species differences in the development of diet-induced obesity and metabolic disturbances in rodents. Front Nutr 9:828522.

McMahon LR, Wellman PJ (1998) PVN infusion of GLP-1-(7-36) amide suppresses feeding but does not induce aversion or alter locomotion in rats. Am J Physiol 274:R23–R29.

Mella R, Schmidt CB, Romagnoli PP, Teske JA, Perez-Leighton C (2017) The food environment, preference, and experience modulate the effects of exendin-4 on food intake and reward. Obesity (Silver Spring) 25:1844–1851.

Merchenthaler I, Lane M, Shughrue P (1999) Distribution of pre-pro-glucagon and glucagon-like peptide-1 receptor messenger RNAs in the rat central nervous system. J Comp Neurol 403:261–280.

Mul JD, Begg DP, Barrera JG, Li B, Matter EK, D'Alessio DA, Woods SC, Seeley RJ, Sandoval DA (2013) High-fat diet changes the temporal profile of GLP-1 receptor-mediated hypophagia in rats. Am J Physiol Regul Integr Comp Physiol 305:R68–R77.

Ong ZY, Liu JJ, Pang ZP, Grill HJ (2017) Paraventricular thalamic control of food intake and reward: role of glucagon-like peptide-1 receptor signaling. Neuropsychopharmacology 42:2387– 2397.

Paxinos G, Franklin K (2000) The mouse brain in stereotaxic coordinates. 2nd ed. San Diego: Academic.

Reiner DJ, Mietlicki-Baase EG, McGrath LE, Zimmer DJ, Bence KK, Sousa GL, Konanur VR, Krawczyk J, Burk DH, Kanoski SE, Hermann GE, Rogers RC, Hayes MR (2016) Astrocytes regulate GLP-1 receptor-mediated effects on energy balance. J Neurosci 36:3531– 3540.

Reiner DJ, Leon RM, McGrath LE, Koch-Laskowski K, Hahn JD, Kanoski SE, Mietlicki-Baase EG, Hayes MR (2018) Glucagon-like peptide-1 receptor signaling in the lateral dorsal tegmental nucleus regulates energy balance. Neuropsychopharmacology 43:627–637.

Richard JE, Farkas I, Anesten F, Anderberg RH, Dickson SL, Gribble FM, Reimann F, Jansson JO, Liposits Z, Skibicka KP (2014) GLP-1 receptor stimulation of the lateral parabrachial nucleus reduces food intake: neuroanatomical, electrophysiological, and behavioral evidence. Endocrinology 155:4356–4367.

Richard JE, Anderberg RH, López-Ferreras L, Olandersson K, Skibicka KP (2016) Sex and estrogens alter the action of glucagon-like peptide-1 on reward. Biol Sex Differ 7:6.

Rinaman L (2010) Ascending projections from the caudal visceral nucleus of the solitary tract to brain regions involved in food intake and energy expenditure. Brain Res 1350:18–34.

Sadacca BF, Rothwax JT, Katz DB (2012) Sodium concentration coding gives way to evaluative coding in cortex and amygdala. J Neurosci 32:9999–10011.

Sadacca BF, Mukherjee N, Vladusich T, Li JX, Katz DB, Miller P (2016) The behavioral relevance of cortical neural ensemble responses emerges suddenly. J Neurosci 36:655–669.

Salinero AE, Anderson BM, Zuloaga KL (2018) Sex differences in the metabolic effects of diet-induced obesity vary by age of onset. Int J Obes (Lond) 42:1088–1091.

Samuelsen CL, Vincis R (2021) Cortical hub for flavor sensation in rodents. Front Syst Neurosci 15:772286.

Saper CB (2002) The central autonomic nervous system: conscious visceral perception and autonomic pattern generation. Annu Rev Neurosci 25:433–469.

Small DM, Zatorre RJ, Dagher A, Evans AC, Jones-Gotman M (2001) Changes in brain activity related to eating chocolate: from pleasure to aversion. Brain 124:1720–1733.

Small DM, Gregory MD, Mak YE, Gitelman D, Mesulam MM, Parrish T (2003) Dissociation of neural representation of intensity and affective valuation in human gustation. Neuron 39:701–711.

Stapleton JR, Lavine ML, Wolpert RL, Nicolelis MAL, Simon SA (2006) Rapid taste responses in the gustatory cortex during licking. J Neurosci 26:4126–4138.

Stern SA, Doerig KR, Azevedo EP, Stoffel E, Friedman JM (2020) Control of non-homeostatic feeding in sated mice using associative learning of contextual food cues. Mol Psychiatry 25:666–679.

Stern SA, Azevedo EP, Pomeranz LE, Doerig KR, Ivan VJ, Friedman JM (2021) Top-down control of conditioned overconsumption is mediated by insular cortex Nos1 neurons. Cell Metabolism 33:1418–1432.e6.

Swick JC, Alhadeff AL, Grill HJ, Urrea P, Lee SM, Roh H, Baird JP (2015) Parabrachial nucleus contributions to glucagon-like peptide-1 receptor agonist-induced hypophagia. Neuropsychopharmacology 40:2001–2014.

Tang-Christensen M, Larsen PJ, Göke R, Fink-Jensen A, Jessop DS, Møller M, Sheikh SP (1996) Central administration of GLP-1-(7-36) amide inhibits food and water intake in rats. Am J Physiol 271:R848–R856.

Tauchi M, Zhang R, D'Alessio DA, Stern JE, Herman JP (2008) Distribution of glucagon-like peptide-1 immunoreactivity in the hypothalamic paraventricular and supraoptic nuclei. J Chem Neuroanat 36:144–149.

Terrill SJ, Holt MK, Maske CB, Abrams N, Reimann F, Trapp S, Williams DL (2019) Endogenous GLP-1 in lateral septum promotes satiety and suppresses motivation for food in mice. Physiol Behav 206:191–199.

Thiebaud N, Llewellyn-Smith IJ, Gribble F, Reimann F, Trapp S, Fadool DA (2016) The incretin hormone glucagon-like peptide 1 increases mitral cell excitability by decreasing conductance of a voltage-dependent potassium channel. J Physiol 594:2607–2628.

Unger RH, Eisentraut AM (1969) Entero-Insular Axis. Arch Intern Med 123:261–266.

Van Bloemendaal L, IJzerman RG, Ten Kulve JS, Barkhof F, Konrad RJ, Drent ML, Veltman DJ, Diamant M (2014) GLP-1 receptor activation modulates appetite- and reward-related brain areas in humans. Diabetes 63:4186–4196.

Vincis R, Chen K, Czarnecki L, Chen J, Fontanini A (2020) Dynamic representation of taste-related decisions in the gustatory insular cortex of mice. Curr Biol 30:1834–1844.e5.

Vrang N, Phifer CB, Corkern MM, Berthoud HR (2003) Gastric distension induces c-Fos in medullary GLP-1/2-containing neurons. Am J Physiol Regul Integr Comp Physiol 285:R470–R478.

Vrang N, Hansen M, Larsen PJ, Tang-Christensen M (2007) Characterization of brainstem preproglucagon projections to the paraventricular and dorsomedial hypothalamic nuclei. Brain Res 1149:118–126.

Wang F, Flanagan J, Su N, Wang LC, Bui S, Nielson A, Wu X, Vo HT, Ma XJ, Luo Y (2012) RNAscope: a novel in situ RNA analysis platform for formalin-fixed, paraffin-embedded tissues. J Mol Diagn 14:22–29.

Wilding JPH, Batterham RL, Calanna S, Davies M, Van Gaal LF, Lingvay I, McGowan BM, Rosenstock J, Tran MTD, Wadden TA, Wharton S, Yokote K, Zeuthen N, Kushner RF (2021) Once-weekly semaglutide in adults with overweight or obesity. N Engl J Med 384:989–1002.

Williams DL (2022) The diverse effects of brain glucagon-like peptide 1 receptors on ingestive behaviour. Br J Pharmacol 179:571– 583.

Williams DL, Hyvarinen N, Lilly N, Kay K, Dossat A, Parise E, Torregrossa AM (2011) Maintenance on a high-fat diet impairs the anorexic response to glucagon-like-peptide-1 receptor activation. Physiol Behav 103:557–564.

Williams EKK, Chang RBB, Strochlic DEE, Umans BDD, Lowell BBB, Liberles SDD (2016) Sensory neurons that detect stretch and nutrients in the digestive system. Cell 166:209–221.

Wu Y, Chen C, Chen M, Qian K, Lv X, Wang H, Jiang L, Yu L, Zhuo M, Qiu S (2020) The anterior insular cortex unilaterally controls feeding in response to aversive visceral stimuli in mice. Nat Commun 11:1–14.

Yasui Y, Breder CD, Safer CB, Cechetto DF (1991) Autonomic responses and efferent pathways from the insular cortex in the rat. J Comp Neurol 303:355–374.

Zeng N, Cutts EJ, Lopez CB, Kaur S, Duran M, Virkus SA, Hardaway JA (2021) Anatomical and functional characterization of central amygdala glucagon-like peptide 1 receptor expressing neurons. Front Behav Neurosci 15:337.

Zhang C, Wu B, Beglopoulos V, Wines-Samuelson M, Zhang D, Dragatsis I, Sdhof T, Shen J (2009) Presenilins are essential for regulating neurotransmitter release. Nature 460:632–636.

Zhang-Molina C, Schmit MB, Cai H (2020) Neural circuit mechanism underlying the feeding controlled by insula-central amygdala pathway. iScience 23:101033.